EFFECT OF ELECTRIC-FIELD PERTURBATIONS NEAR THE ANODE ON THE OSCILLATIONS ON A PENNING DISCHARGE

G. V. Smirnitskaya, E. M. Reikhrudel, and I. A. Nosyreva

Vestnik Moskovskogo Universiteta. Fizika, Vol. 25, No. 3, pp. 285-292, 1970

UDC 537.525

In an attempt to determine the nature of the oscillations which arise in a Penning discharge, a study has been made of the role played by perturbations caused in the electric field near the anode by longitudinal apertures in the cylindrical anode. The radial potential drop was measured by the "ion-kinetics" method. A study was also made of the sensitivity of the discharge oscillations to the potential on probes placed in the anode apertures.

The oscillations which arise in a discharge with crossed electric and magnetic fields, due to an instability of the electron space charge near the anode, were studied in [1-4]. In strong magnetic fields ($H>400$ Oe) and at low pressures ($p<10^{-4}$torr), a rotating sheath of negative space charge forms near the anode surface in a cold-cathode Penning discharge. The thickness of this sheath decreases with increasing H; at a certain thickness, the sheath becomes unstable, and inhomogeneities ("spokes") arise and produce oscillations. The thinner the layer, the more intense the spoke formation, and the higher the oscillation mode. It was shown in [6] that the spoke formation is due to conditions at the sheath boundary, so some agent which affects the electron sheath near the anode should be reflected in the oscillations of this sheath. It was shown in [4] that a probe parallel to the axis and inserted at a certain depth (2-3 mm from the anode) can intercept the electron sheath and alter the oscillation mode.

EXPERIMENTAL PROCEDURE AND RESULTS

We report here a study of the effects of perturbations caused in the electric field near an anode by longitudinal apertures (slits) on the oscillations of the electron sheath in a Penning discharge. Under certain discharge conditions, the radial potential drop has different values in cells with and without anode slits. The differences reflected in the oscillation frequency, and the oscillation intensity is greater when there are slits. It is also shown that a perturbation of the electric field caused by supplying a negative voltage (with respect to anode) to probes in the anode slits leads to oscillations whose mode and intensity depend on the nature and degree of the field perturbation.

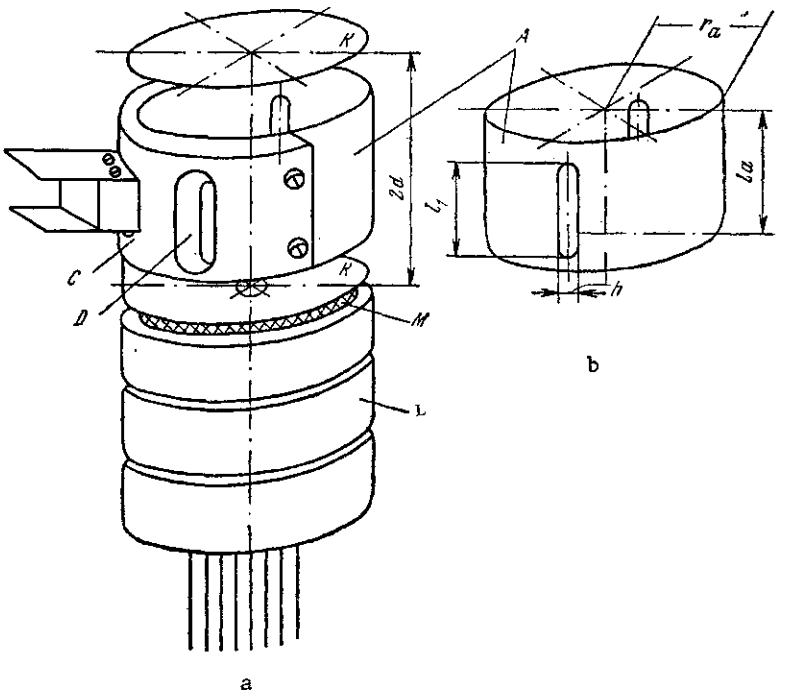

Fig. 1. a) Discharge cell with a replaceable anode; b) anode with two slits.

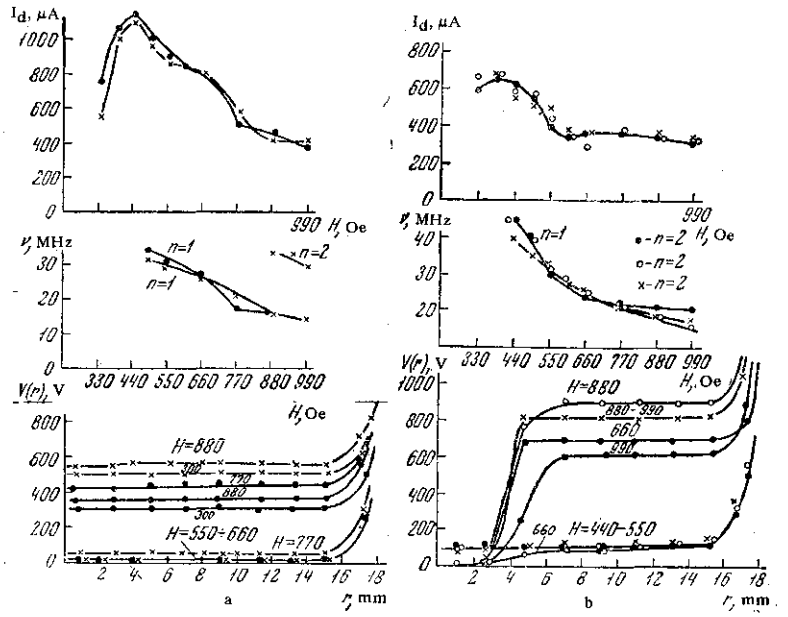

Fig. 2. $I_d=f(H)$, $\nu=f(H)$ and $V(r)=f(r)$ curves for cells having various anode configurations. a) V_a = 1000 V, p = 1 · 10^{-4} torr, r_a=1,25 cm, l_a=2,5 cm, $2d$=4 cm, l_1=1,7 cm, h=0,27 cm] ●) solid anode; ○) anode with four slits]; b) V_a = 2000 V, p = 5 · 10^{-5} torr, r_a=1,85 cm, l_a=2,5 cm, $2d$=4 cm, l_1=1,7 cm, h=0,4 cm,] ●) solid anode; ×) anode with two slits; ○) anode with four slits].

Figure 1 shows the construction of a discharge cell. Cylindrical anodes of various diameters, both solid and having longitudinal slits, are placed in a holder C. The measurements are carried out with anodes having one, two, or four slits arranged symmetrically, with respect to the anode axis. The slit dimensions are indicated in the figures and tables. The holder also has large apertures D to reduce the effect of the holder on the discharge. As the center of one of the cathalists there is an aperture symbol for of the order of 0.25 cm in diameter, used to measure the radial potential drop on the basis of the maximum ion energy by means of a sectioned collector L [5]. Grid M, supplied a potential for about − 100 V, is used to retard electrons and prevent them from interfering. Finally, A is the replaceable anode, and K are the cathodes.

The radial potential drop measured with slits present does not reflect the perturbations caused in the field by the slits, but it permits an estimate to be made of the effect of the slits on the ionization in discharge and on the space-charge density. The oscillation frequency is measured by an S4-8 spectrum analyzer, which analyzes the voltage across a resistance in the cathode circuit.

Figure 2 shows dependences of the discharge current I_d, the oscillation frequency ν, and the radial potential drop V(r) on the magnetic field H for cells having solid cylindrical anodes and for cells having anodes having various numbers of slits, for two values of each of the parameters r_a, V_a and p. The results obtained of the anode having a single slit approximate those obtained with the solid anode. The discharge currents in these cells having a different type of anode are seen to be approximately the same. At H the oscillation frequency in the cells with the solid anodes (ν_s) is slightly higher than that (ν_h) in the cells having anodes with slits. As H increases, ν_h becomes greater than ν_s, but at even greater H we again find $\nu_s > \nu_h$.

Study of the radial potential drop $V_a - V_0$ reveals an explanation for the H dependence of the frequency for the different anode geometries. With small H in the cells with the solid anodes, $V_a - V_0$ is higher than in the cells having the anodes with slits. This apparently occurs because in the presence of slits the field perturbations near the anode cause some of the electrons to move along trajectories which are not closed; these electrons cause less ionization, with the density of the negative space charge in solids with such anodes decreases (H = 330 Oe, Fig. 2a). The oscillation frequency is

$$\nu = n\frac{c(V_a - V_0)}{\pi H r_a^2}, \quad n = 1, 2, 3 \qquad (1)$$

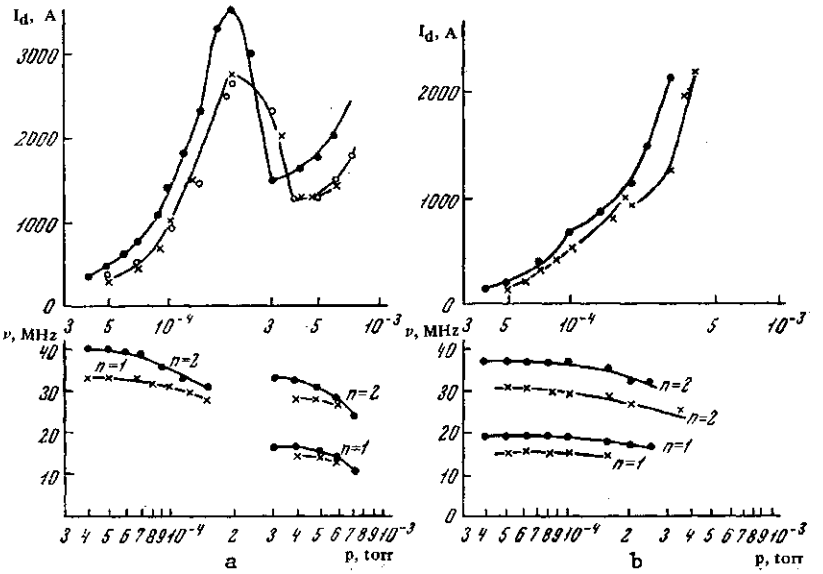

Fig. 3. $I_d=f(p)$, $\nu=f(p)$ curves for cells having different anode configurations, for two values of H, but for otherwise equal conditions) V_a = 1500 V, r_a=1,85 cm, l_a=2,5 cm, $2d$=4 cm, l_1=1,7 cm, h=0,4 cm;). a) H = 330 Oe; •) solid anode; ×) anode with two slits; ○) anode with four slits; h) H = 770 Oe, •) solid anode; ×) anode with two slits.

and decreases with decreasing (V_a-V_0). With a further increase in H, (V_a-V_0) increases, reaching a maximum $V_a-V_0=V_a$ at some H. The oscillation frequencies at these H values are approximately the same for the cells having the different anode configurations. (H = 500-660 Oe, Fig. 2). As the axial potential drop increases, the rate at which ions move toward the cathode becomes comparable to the rate at which electrons move toward the anode. A positive space charge begins to affect the potential distribution and thus the oscillation frequency. When slits are present, the frequency ν_i at which ionization is caused by electrons in these slits is less, so fewer ions are formed near the slits ($n_i=\nu_i n_e$). The total density of the positive space charge in the cell with the anode having slits is less and may not be sufficient to balance the negative space charge. For this reason, a positive space charge appears at a smaller H in the cell having the solid anode, V_a-V_0 falls off rapidly, and the ν_s becomes smaller than ν_h. As H increases in the cell in which the anode has slits, there is an increase in the number of electrons moving along closed trajectories and thus in the rate of ionization caused by these electrons in the slits. At some H we have $n_e\simeq n_i$, and a positive space charge also arises in the cells in which the anodes have slits; this appearance is accompanied by decreases in V_a-V_0 and ν. With a further increase in H in the solid-anode cells, ionization by the faster electrons and by the electrons formed far from the axis again is accompanied by an increase in V_a-V_0 and in ν_s, which becomes greater than ν_h. The oscillation frequency under these conditions is

$$\nu = n\frac{c(V_a-V_{01})}{\pi H (r_a-r_{01})^2}, \qquad (2)$$

where V_{01} is the potential and r_{01} is the boundary of the virtual cathode which arises near the axis.

Table 1 shows the measured (V_a-V_0), (r_a-r_{01}), and ν_{expt} values, along with the frequencies ν_{theo} calculated from Eqs. (1) and (2). As the number of slits increases, the radiation intensity W increases, apparently because when there are slits present a greater number of electrons combine into spokes.

Figure 3 shows $I_d=f(p)$, $\nu=f(p)$ curves for two values of H, for cells with and without anode slits. In the cells with the slits, the current jumps and the transition to the plasma regime occur at larger P (Fig. 3a); again an explanation can be found in the smaller of n_i in the cell having the slits. The transition from the plasma regime to that with a negative space charge is accompanied by an abrupt change in (V_a-V_0) and in the oscillation frequency.

At larger H the reduction of the axial potential drop V_0 leads to an increased effect of the positive

space charge. The current jump on the $I_d=f(p)$ becomes less pronounced, and the oscillation frequency changes smoothly (Fig. 3b). Table 2 compares the experimental ν values for various p with those calculated with an account of (V_a-V_0).

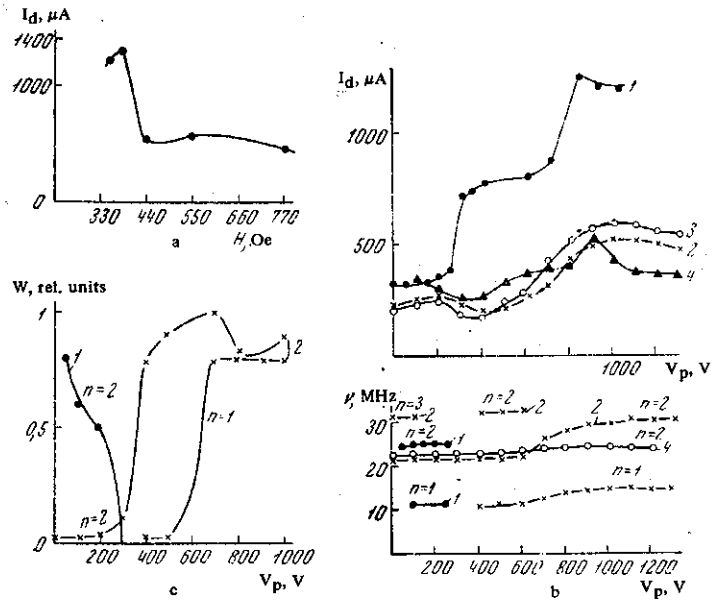

Fig. 4. Effects on the discharge current and on the oscillations of perturbations caused in the electric field near the anode by a probe. Here $r_a=1{,}85$ cm, $l_a=2{,}5$ cm, $2d=4$ cm, $l_1=1{,}7$ cm, $h=0{,}4$ cm. a) $I_d = f(H)$ for $V_p = V_a$; $I_d = f(V_p)$ and $\nu = f(V_p)$ for various H. 1) H = 360 Oe; 2) 440; 3) 550; 4) 770. c) dependence of the oscillation amplitude on V_p for two values of H. 1) 360; 2) 400 Oe.

To determine the effect of field perturbations near the anode on the current oscillations, we also carried out experiments in which we placed probes in the anode slits. The probes were planar and reproduced the slit shape. They were held at potentials ranging from zero to V_a. Figure 4a shows an $I_d=f(H)$ curve for a probe potential $V_p=V_a$, where Fig. 4b shows the dependences of the discharge current and oscillation frequency on the probe potential for various H. As V_p increases (with respect to the cathode potential), the discharge current increases, since a greater number of electrons are moving along closed trajectories and thus a greater number are causing ionization. Figure 4c shows $W=f(V_p)$ dependences for various H. At small H (360 Oe), at which the discharge current increases with increasing H (for $V_p=V_a$), oscillations are not observed in the discharge (discharge regime I [7]). In this regime the negative space charge is distributed uniformly near the anode. However, when the large negative potential is supplied to the probes at these H values, the field within the anode becomes disturbed, and the uniformity of space charge distribution is disrupted. Where the field is disrupted by the probe potentials, electrons accumulate, a spoke forms in the discharge, and oscillations appear. As V_p is increased, the discruption of the field by the probes is reduced, the nonuniformity of the azimuthal density distribution disappears, and the oscillations disappear at small H. When probes in two slits are held in negative potentials, the second harmonic is much greater than the first at small H (Fig. 4c, H = 360 Oe), apparently because the trajectories of most of the electrons are perturbed at two points. At larger H, in discharge regime II (on the descending $I_d = f(H)$), the azimuthal distribution of electrons in the discharge is nonuniform, and oscillations are observed at all probe potentials. An increase in V_p in accompanied by a gradual increase in the frequency.

Table 3 shows that the radial potential drop increases as V_p increases, since there is an increase in the rate of ionization by electrons moving along closed trajectories. The result is an increase in the oscillation frequency. At V_p the amplitude of the second harmonic is greater than that of the first, but as V_p increases, the amplitude of the two harmonics become comparable (Fig. 4c).

Table 1

V_a=1000 V p=1·10⁻⁴ torr r_a=1,25 cm l_a=2,5 cm 2d=4 cm

	Solid anode					Anode with four slits, ℓ_1 = 1.7 cm, h = 0.27 cm				
H, Oe	(V_a-V_{a1}), V	(r_a-r_{a1}), cm	ν_{expt} MHz	ν_{reop}, MHz	W, mm	(V_a-V_{a1}), V	(r_a-r_{a1}), cm	ν_{expt} MHz	ν_{theo} MHz	W, mm
495	980	1,25	32	40	2	950	1,25	31	40	20
660	980	1,25	28,5	30	1	990	1,25	27	30	15
770	570	1,19	17,3	16,8	2	930	1,25	21	24	10
880	570	1,1	16,5	16,2	1	460	1,05	16,5	15,6	60
								33	31,2	5

V_a=2000 V p=5·10⁻⁵ torr r_a=1,85 cm l_a=2,5 cm 2d=4 cm

	Solid anode					Anode with four slits ℓ_1 = 1.7 cm, h = 0.4 cm					Anode with two slits ℓ_1 = 1.7 cm, h = 0.4 cm				
H, Oe	(V_a-V_{a1}), V	(r_a-r_{a1}), cm	ν_{expt} MHz	ν_{theo} Mhz	W, mm	(V_a-V_{a1}), V	(r_a-r_{a1}), cm	ν_{expt} MHz	ν_{theo} MHz	W, mm	(V_a-V_{a1}), V	(r_a-r_{a1}), cm	ν_{expt} MHz	ν_{theo} MHz	W, mm
440	1900	1,85	42	40	40	1900	1,85	36	40	100	1900	1,85	45	40	150
550	1900	1,85	29,5	32	20	1900	1,85	32	32	800	1950	1,85	31	32	5000
660	1320	1,61	24	24,5	1	1940	1,85	25,6	26,7	500	1900	1,85	25	26,7	1500
770	1580	1,61	22	24	10	1940	1,85	20,2	22,7	100	1250	1,61	21	20	4000
880	1420	1,56	21,5	21	25	1200	1,52	18,7	19	100	1070	1,47	18,5	18	2000
990	1340	1,56	19	20	40			16,8	16,8	400	1150	1,47	16,2	17	800
			40	40	15	1200	1,52	33	33	300			32	34	800

Table 2

V_a=1500 V r_a=1,85 cm l_a=2,5 cm H=330 Oe

	Solid anode				Anode with two slits l_1=1,7 cm h=0,4 cm			
p, torr	(V_a-V_{a1}), V	(r_a-r_{a1}), cm	ν_{expt} MHz	ν_{theo} MHz	(V_a-V_{a1}), V	(r_a-r_{a1}), cm	ν_{expt} MHz	ν_{theo} MHz
4·10⁻⁴	500	1,85	16,4	14	570	1,85	15	16
			32	28			28	32
1·10⁻⁴	1280	1,85	35	35,5	1140	1,85	31	32
5·10⁻⁵	1310	1,76	40	41	1270	1,85	33	36

V_a=1500 V r_a=1,85 cm l_a=2,5 cm H=770 Oe

	Solid anode				Anode with two slits l_1=1,7 cm h=0,4 cm			
p, torr	(V_a-V_{a1}), V	(r_a-r_{a1}), cm	ν_{expt} MHz	ν_{theo} MHz	(V_a-V_{a1}), V	(r_a-r_{a1}), cm	ν_{expt} MHz	ν_{theo} MHz
2·10⁻⁴	680	1,32	16	16	850	1,66	14	12,8
			32	32			28	25,6
1·10⁻⁴	1000	1,47	18,6	18,9	880	1,52	15,7	15,8
			37	37,8			31	31,6
5·10⁻⁵	1180	1,47	18,7	19,3	880	1,52	16	15,8
			37	38,6			31	31,6

Table 3

V_a=1000 V p=1·10⁻⁴ torr r_a=1,85 cm l_a=2.5 cm 2d=4 cm l_1=1,7 cm h=0,4 cm

	V_3=0				V_3=V_a			
H, Oe	(V_a-V_{a1}), V	(r_a-r_{a1}), cm	ν_{expt} MHz	ν_{theo} MHz	(V_a-V_{a1}), V	(r_a-r_{a1}), cm	ν_{expt} MHz	ν_{theo} MHz
385	480	1,85	23	11,5	900	1,85	19,5	22
			32	23			36	44
				34,5				
440	500	1,85	21	10,5	620	1,61	16	17
			31,5	21			32	34
				31,5				
550	370	1,66	16,5	7,8	650	1,56	14,5	15,5
			26,5	15,6			29	31
				23,4				
770	390	1,32	22	9,4	530	1,3	12	12,5
				18,8			24	25

REFERENCES

1. W. Knauer, Journ. Appl. Phys., 33, No. 6, 2093, 1962; 37, No. 2, 602, 1966.
2. I. C. Helmer and R. L. Jepsen, Proc. I R E., 49, No. 12, 1966.
3. A. Raev, I. Iliev, and N. Nikolov, 8-th Internat. Confer. on Phenom. in Ioniz. Gases, Vienna, 186, 1967.
4. E. N. Hirsch, Brit. J. Appl. Physics., 15, 1535, 1964.
5. E. M. Reikhrudel, G. V. Smirnitskaya, and R. P. Babertsyan, ZhTF, 36, no. 7, 1226, 1966.
6. R. H. Gevy, Phys. of Fluids., 8, No. 7, 1288, 1965; 11, No. 4, 773, 920, 1968.
7. E. M. Reikhrudel, G. V. Smirnitskaya, and Nguen Khyu Ti, ZhTF, 39, no. 6, 1052, 1969.

4 June 1969

Department of General Physics for the Natural Sciences